Available online at www.sciencedirect.com
SCIENCE DIRECT
ELSEVIER
Composites Science and Technology 64 (2004) 711–717
COMPOSITES SCIENCE AND TECHNOLOGY
www.elsevier.com/locate/compscitech

Unstable crack advance across a regular array of short fibers in brittle matrix

Yu Qiao*, Xinguo Kong

Department of Civil Engineering, University of Akron, Akron, OH 44325-3905, USA

Received 14 May 2003; received in revised form 12 July 2003; accepted 21 July 2003

Abstract

The resistance to cleavage cracking of a regular array of short fibers was discussed through *R*-curve analysis. The final failure of the fiber array associated with the unstable crack advance across it occurred when the balance of the rates of the energy release rate and the fracture resistance was reached. The fracture resistance dominated by the combined bridging effect and crack trapping effect increased with the volume fraction and the aspect ratio of the fibers, as well as the internal friction. The toughening effect strongly depended on the crack length for short cracks but was size insensitive for long cracks. The elastic properties of the matrix had little influence on the overall fracture resistance.

Keywords: A. Short-fiber composites; B. Fracture toughness; C. Failure criterion; C. Fiber bridging

1. Introduction

For many decades short fiber reinforced composites (SFRC) based on polymeric, metallic, and ceramic materials have been widely applied due to the advanced mechanical and thermal properties, as well as the cost efficient processing. One of the most important features of SFRC is the high fracture resistance. Various toughening mechanisms such as the bridging effect and the crack trapping effect were investigated both experimentally and numerically [1–5].

In engineering practice where the reliable service performance of the composites must be assured under any adverse condition, understanding the process of cleavage cracking across the short fibers was of great interest. At relatively low temperature, in intrinsically brittle or quasi-brittle matrix the fracture mode is cleavage, which can be studied in context of linear elastic fracture mechanics (LEFM) quite successfully. In this theory the driving force of the crack advance is described by a single parameter K, the stress intensity factor, or, equivalently, G, the energy release rate. When the dissipation rate of the strain energy and the work of separation of the fracture surfaces are equal to each other, i.e.

$$G = R, \tag{1}$$

the crack starts to propagate, with R being the fracture resistance of the material.

In many SFRC, the fiber–matrix interface could not survive the stress concentration at the crack tip. Debonding and pull-out of the short fibers from the matrix were repeatedly reported in both laboratory tests and field applications [6–9]. The mechanics of the advance of the cleavage crack in such a composite with a process zone behind the crack tip where a characteristic traction separation process is dominant has been considered in detail by Andersson and Bergkvist [10]. The traction process was assumed to be linear and the fracture resistance of the composite was modeled through area average

$$G_{\text{composite}} = n\left(\hat{\sigma}\hat{\delta}/2\right) \tag{2}$$

where n is the number density per unit width of the short fibers, $\hat{\sigma}$ is the peak traction force, and $\hat{\delta}$ is the maximum traction distance above which the traction force becomes negligible. Although this model, as well

* Corresponding author. Tel.: +1-330-972-2426; fax: +1-330-972-6020.

E-mail address: yqiao@uakron.edu (Y. Qiao).

0266-3538/$ - see front matter
doi:10.1016/j.compscitech.2003.07.001

as the *R*-curve analyses based on it, has been of unquestionable utility, the crack front–fiber interaction could not be accounted for. As will be discussed below, the penetration process of the crack front across an array of short fibers consists of the stable crack growth and the unstable crack advance. The crack growth becomes unstable before the fibers are fully pulled out. Thus, Eq. (2) somewhat overestimated the toughening effect by assuming that the pull-out process was complete and, on the other hand, tended to underestimate the toughening effect since the non-uniform nature of the cleavage front profile was ignored.

Fig. 1 [11] shows the evolution of the cleavage front profile in an epoxy resin reinforced by a regular array of well-boned nylon rods. When the cleavage front encountered the obstacles it first penetrated between them stably. The obstacles bridged across the two crack flanks and trapped the cleavage front locally. According to Eq. (1), the stress intensity along the verge of propagating was equal to the resistance of the matrix, while that along the nylon rods should be larger. Consequently, the overall stress intensity at the crack tip was higher than K_{IC}^{matrix}, the critical stress intensity factor of the matrix. If the obstacles were tough enough and the obstacle–matrix interface was perfect, eventually the

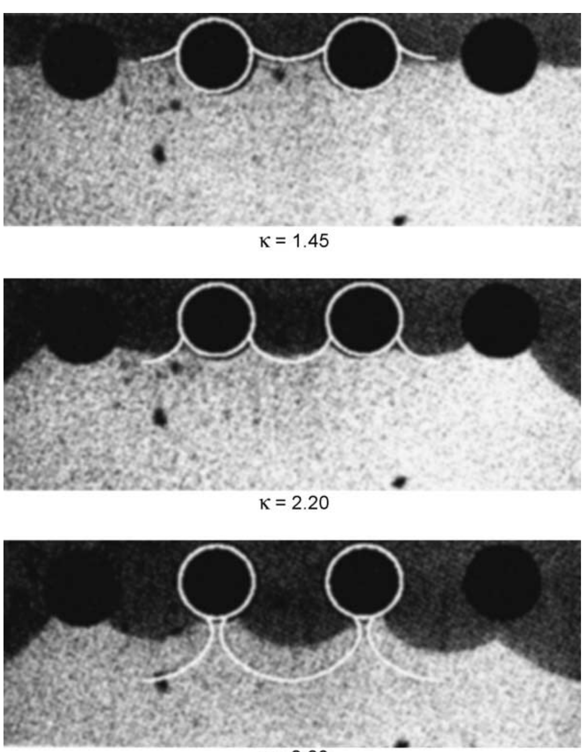

Fig. 1. The evolution of the profile of the cleavage front overcoming the crack trapping effect of a regular array of well-bonded nylon rods in epoxy matrix [11]. The effective crack-tip stress intensities are indicated by $\kappa = K_I^{eff}/K_{IC}^{matrix}$, with K_I^{eff} being the applied stress intensity. The white lines are the numerical results provided by Bower and Ortiz [14].

crack front would surround the obstacles somewhat similar to a dislocation line bypassing precipitations. This phenomenon has been studied through computer simulations intensively, and the numerical results fit with the experimental data quite well [12–16]. However, in most of these models [12–15] it was assumed that the cleavage front could cut through the obstacles gradually, which made it difficult to take account for the fiber–matrix debonding.

In the following discussion we will analyze the resistance of a regular array of debondable, tough short fibers to cleavage cracking through *R*-curve method. If the volume fraction of the fibers is low or the maximum traction displacement is small, the resistance of the fibers exposed in the fracture surface has been fully overcome before the crack front encounters the next fiber array. Under this condition the resistance offered by a single array of short fibers is dominant to the overall fracture toughness. If more than one arrays are involved in the crack front advance, process-zone model based on understanding the single array behavior should be developed, which is important but beyond the scope of this paper.

2. Resistance curve of a regular array of short fibers

As discussed above, in many SFRC the fibers can be pulled out when the cleavage front bypasses them. Additional fracture work is required to overcome the bridging effect as well as the crack trapping effect. In the pure bending test of chopped strand mat and sheet molding compound materials [8], it was found that the bridging behavior was independent to the specimen geometry. Therefore, the bridging law should be taken as a material property.

The separation of the fibers from the matrix can be considered as the mixed-mode fracture triggered by "preparatory" shear deformation, after which the internal friction between the fibers and the matrix is constant. Consider the crack front depicted in Fig. 2a. The material is homogeneous elsewhere except for the regular array of the short fibers. When the stress intensity at the crack tip is higher than K_{IC}^{matrix}, the front starts to penetrate between the fibers stably. Debonding occurs along the fiber–matrix interface if the required bridging force exceeds the critical value

$$f_b = k(2\pi r)(h_0 - \Delta h) \tag{3}$$

where k is the effective work of separation of the fiber–matrix interface, Δh is the crack opening displacement along the short fibers, and r and h_0 are the radius and the half length of the fibers, respectively. With increasing stress intensity the penetration depth of the crack front increases (see Fig. 2b), which results in the well-known *R*-curve. Note that due to the nonuniform nature of the crack front profile, the effective crack growth distance

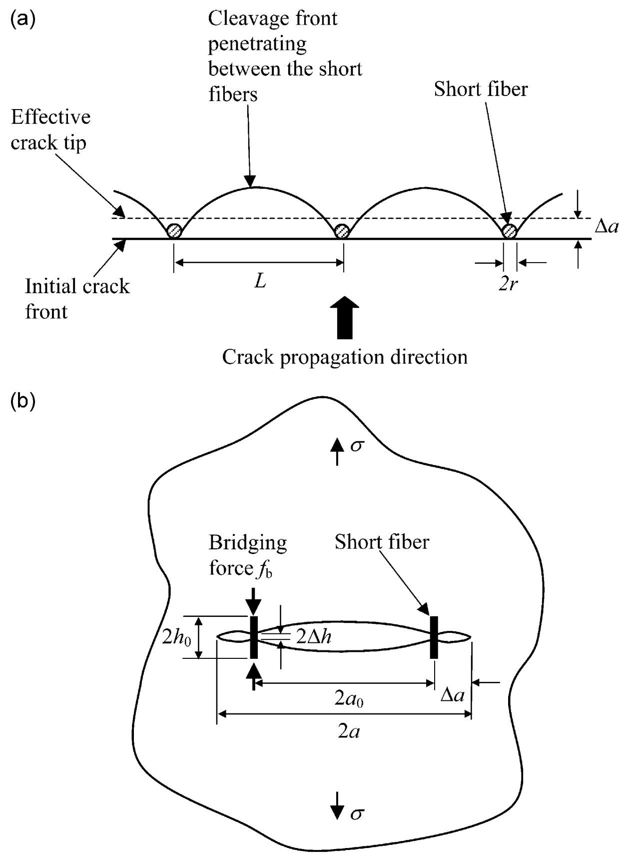

Fig. 2. Schematic diagram of cleavage cracking across a regular array of short fibers: (a) top view; (b) side view.

Δa should be smaller than the maximum penetration depth of the verge of propagating.

Fig. 3 shows a typical R-curve. For the crack depicted in Fig. 2b, with the constant applied stress σ, the energy release rate increases with crack length. If σ is small, e.g. when $\sigma = \sigma_1$, the energy release rate is below the fracture resistance of the matrix, G_{matrix}, and the crack length remains the initial value, a_0, until the stress is increased to σ_2, where Eq. (1) is satisfied and the crack starts to grow. Since with the crack advance the fracture resistance increases more rapidly than the energy release rate, the

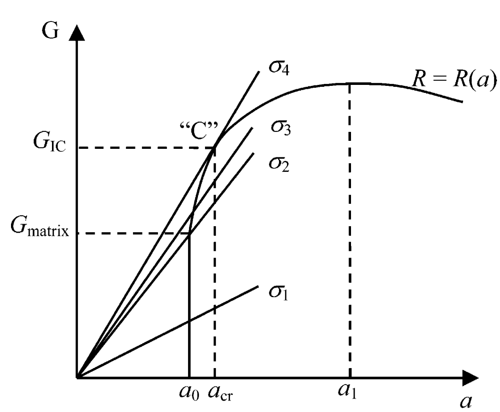

Fig. 3. Schematic diagram of a typical R-curve analysis.

crack will be arrested immediately. The crack grows stably with increasing σ until the crack length a increases to the critical value a_{cr}, where

$$\frac{\partial G}{\partial a} = \frac{\partial R}{\partial a} \tag{4}$$

Then, the crack advance becomes unstable and the final failure occurs.

The stress intensity factor at the tip of the cleavage crack in Fig. 2b caused by the bridging force can be calculated as [17]

$$K_{I0} = \frac{P_0}{\sqrt{\pi a}}\sqrt{1 + 2\frac{a_0}{\Delta a}} \tag{5}$$

where P_0 is the effective bridging force per unit width. The associated strain energy is

$$\frac{U_0}{B} = \frac{1-\nu^2}{E}\frac{P_0^2}{\pi}\ln\frac{1+x}{x^2} \tag{6}$$

where B is the specimen thickness; ν and E are the Poisson's ratio and the Young's modulus of the matrix, respectively; and $x = \Delta a/a_0$. Note that $\Delta a = a - a_0$. Since the response of the matrix is elastic, we have

$$\Delta h^* = \left(\frac{1-\nu^2}{\pi E}\ln\frac{1+x}{x^2}\right)P_0 \tag{7}$$

with Δh^* being the change of the crack opening displacement caused by P_0. If the fiber array is long enough such that the deformation is under the plane strain condition, P_0 can be taken as f_b/L, with L being the average spacing between the short fibers. Thus, through Eqs. (3) and (7),

$$\Delta h = \frac{\left(\Delta h_0 - k_0 h_0 \ln 1 + x/x^2\right)}{\left(1 - k_0 \ln\frac{1+x}{x^2}\right)} \tag{8}$$

where Δh_0 is the crack opening displacement along the short fibers if the bridging force was zero, and $k_0 = 2(1-\nu^2)\frac{k}{E}\frac{r}{L}$. Note that $\Delta h_0 = \Delta h + \Delta h^*$, and can be estimated as [14]

$$\Delta h_0 = \frac{1-\nu}{\mu}\sqrt{\frac{x(1+x)}{2}}\sigma \cdot a_0 \tag{9}$$

where μ is the shear modulus of the matrix. The relationship among Δh_0, Δh, and Δh^* is depicted in Fig. 4.

Consequently, Eq. (8) can be rewritten as

$$\Delta h = \frac{\left(1 - \nu/\mu\sqrt{\frac{x(1+x)}{2}}\sigma \cdot a_0 - k_0 h_0 \ln\frac{1+x}{x^2}\right)}{\left(1 - k_0 \ln\frac{1+x}{x^2}\right)} \tag{10}$$

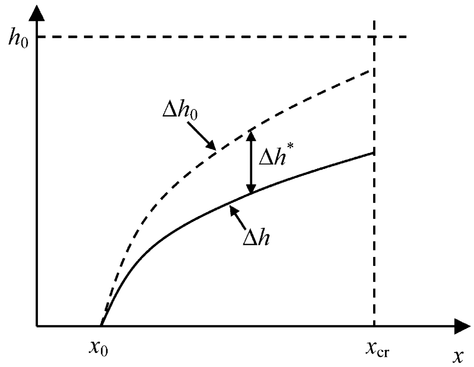

Fig. 4. Schematic diagram of the relationship between the sliding distance along the fiber–matrix interface, Δh, and the normalized effective crack growth length, x, with $x_{cr} = a_{cr}/a_0$. At x_0, the debonding of the fiber–matrix interface occurs. At x_{cr}, before the fibers are fully pulled out, the crack growth becomes unstable, i.e. $\Delta h < h_0$.

Through Eq. (10), we can obtain the critical effective crack growth distance, x_0, at which

$$\Delta h = 0.$$

As discussed above, the effective crack growth distance x increases with the external stress. When x is below x_0, the fiber–matrix interface does not fail. When x reaches x_0, the fibers will be pulled out gradually associated with the stable crack growth. Since the crack breaks through the fibers after the debonding occurs, in the following discussion we only consider the situation where $x > x_0$.

The fracture work associated with the effective crack growth of Δa consists of the work of separation of the matrix and the traction work:

$$W_f = G_{\mathrm{matrix}}\Delta x + \frac{1}{L}[k(2\pi r)(h_0 - \Delta h) + k(2\pi r)h_0]\cdot \Delta h \quad (11)$$

Thus, the resistance curve can be stated as

$$R = \frac{W_f}{\Delta x} = G_{\mathrm{matrix}} + \frac{2\pi k r \Delta h}{a_0 L x}(2h_0 - \Delta h) \quad (12)$$

Hence,

$$\frac{\partial R}{\partial a} = \frac{2\pi k r}{a_0^2 L x}\left[2(h_0 - \Delta h)\frac{\partial \Delta h}{\partial x} - \frac{\Delta h}{x}(2h_0 - \Delta h)\right] \quad (13)$$

The value of $\partial R/\partial a$ is positive when Δh is relatively small and, since the length of the load-bearing part of the short fibers keeps decreasing, decreases with x. When the crack length increases to a_1, Δh reaches Δh_1 where $(\partial R/\partial a)_{\Delta h_1} = 0$, after which $\partial R/\partial a$ becomes negative. However, through Fig. 3 it can be seen that the descending part of the R-curve has no influence on the critical condition of the unstable crack advance. Note that in Eq. (12) the toughening effect of the fibers consisting of the bridging effect and the crack trapping effect is considered as a whole. The crack trapping effect comes in by affecting the crack opening displacement.

The strain energy stored in the matrix is caused by both the external stress and the bridging forces. The strain energy associated with the external stress is

$$\frac{U_1}{B} = \frac{U^*}{B} - \frac{(1-\nu^2)\pi}{2E}\sigma^2 a^2 \quad (14)$$

where U^* is the strain energy if the crack did not exist. The part of the strain energy directly caused by the bridging forces is

$$\frac{U_2}{B} = \frac{1}{L}k(2\pi r)(h_0 - \Delta h)(\Delta h_0 - \Delta h) \quad (15)$$

Based on Eqs. (14) and (15), the energy release rate can be obtained as

$$\begin{aligned} G &= -\frac{\partial(U_1/B + U_2/B)}{\partial a} \\ &= \frac{(1-\nu^2)}{E}\pi\sigma^2 a_0(1+x) + \frac{2\pi k r}{a_0 L}\left[(h_0 + \Delta h_0 - 2\Delta h)\right. \\ &\left.\frac{\partial \Delta h}{\partial x} - \frac{(1-\nu)\sigma a_0}{2\sqrt{2}\mu}(h_0 - \Delta h)\frac{1+2x}{\sqrt{x(1+x)}}\right] \end{aligned} \quad (16)$$

Since the strain energy caused by the external stress is proportional to a^2, its contribution to the energy release rate increases linearly with crack length. On the other hand, since the larger the crack growth distance, the less profound the effect of the bridging forces, with increasing a, the component of the energy release rate associated with the bridging effect decreases with a descending rate, which results in the concave G–a curve. Consequently, there must exist a combination of the external stress and the critical crack length at which both Eqs. (1) and (4) are satisfied. This condition, depicted as point "C" in Fig. 3, indicates the onset of the unstable crack advance leading to the final failure of the fiber array.

Substitution Eqs. (12), (13), and (16) into (1) and (4) gives the critical energy release rate of the unstable crack advance across the array of the short fibers, G_{IC}, which is the peak resistance that the fiber array can offer. It can be seen that G_{IC} is a function of $\{r, h_0, L, \nu, k, a_0, E, \mu, G_{\mathrm{matrix}}\}$. Note that for isotropic matrix, $E/\mu = 2(1+\nu)$. The numerical results showed that E and ν had little influence on G_{IC}, which indicates that the toughening effect of the short fibers is somewhat independent to the elastic properties of the matrix. Hence, according to Π theorem [18], we have

$$\tilde{G} = \frac{G_{IC}}{G_{\mathrm{matrix}}} = f\left(c, \rho, \tilde{k}, \tilde{a}\right) \quad (17)$$

where $c = \pi r^2 h_0/L^3$ is the fiber volume fraction, $\rho = h_0/r$ is the aspect ratio of the short fibers, $\tilde{k} =$

$1 + kh_0^2/(G_{\mathrm{matrix}}r)$ reflects the internal friction, $\tilde{a} = a_0/r$ is the normalized initial crack length, and f is a function determined by Eqs. (1) and (4). The effects of these factors will be discussed in detail below.

3. Results and discussion

Fig. 5 shows the comparison of the experimental data and the numerical results of the relationship between $\tilde{G}$ and c. The experimental data were obtained in the fracture tests of the carbon fiber reinforced cement composites (CFRC1) [19], the carbon fiber reinforced polyethersulphone (CFRP) resin [20], and the steel fiber reinforced cement composites (SFRC) [21]. In CFRC1, the fiber aspect ratio was about 10, and it is reasonable to assume that the initial crack length was of the size comparable to the cement particles, which was about 10 times larger than the fiber radius. If the value of $\tilde{k}$ is taken as 11.0, the numerical curve can capture the experimental result quite well. For CFRP, ρ was about 10 and $\tilde{a}$ was in the range of 1000–2000. For the best fit of the numerical solution to the experimental data, $\tilde{k}$ should be around 16.0. In SFRC, the microstructure was somewhat similar to that of CFRC1, while $\tilde{k}$ was about 5.0, which was considerably lower than that of CFRC1. This was consistent with the observation that the adhesion of the carbon fibers was better than that of the steel fibers. Through the definition of $\tilde{k}$, it can be seen that the value of kh_0/G_{matrix} of these composites were in the range of 0.5–2.0 and quite acceptable. Note that in this model, increasing fiber volume fraction is always of a beneficial effect to the fracture toughness. In real composites, usually when the fiber volume fraction is relatively high the fiber–matrix bonding cannot be developed fully. Under this condition, without considering the c dependence of the internal friction, this model is no longer valid.

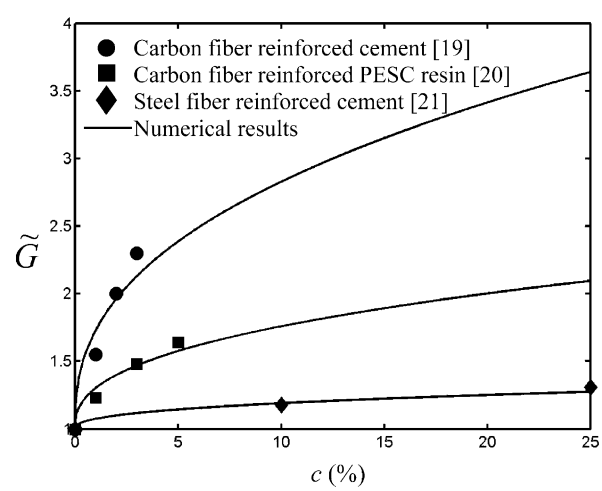

Fig. 5. Comparison of the experimental data and the numerical results of the effect of the fiber volume fraction.

In Andersson–Bergkvist model it was assumed that the fracture resistance of the composite is proportional to the maximum traction distance, which was often related to the fiber length. However, through the numerical result shown in Fig. 6, the $\tilde{G}$–ρ relation is actually nonlinear, as it should. The effect of ρ is quite profound when the fiber is relatively short, while when ρ is larger than 50 its influence becomes negligible. It also can be seen that the stronger the fiber–matrix bonding, the more significant the influence of the fiber length.

As discussed in Section 2, the second derivative of the strain energy is essential to the final failure of the fibers. Therefore, the fracture resistance should be affected by the crack length. On one hand, for a shorter crack, since the crack length dependence of the energy release rate is more profound, the toughness tends to be lower. On the other hand, according to Eq. (12), the fracture resistance of the fibers decreases with the initial crack length. Thus, increasing a_0 tends to lower the fracture resistance. The overall effect of the crack length is shown in Fig. 7. The fracture resistance decreases rapidly with

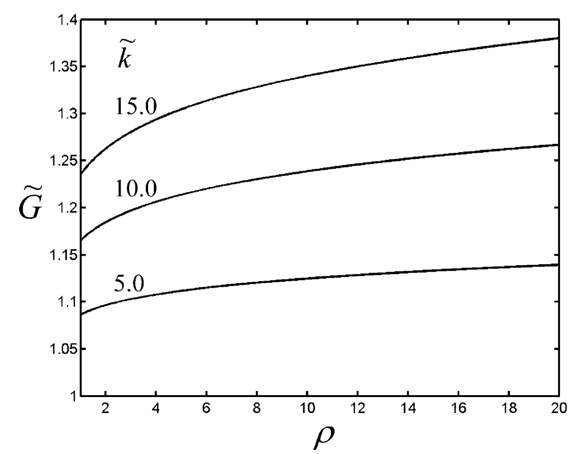

Fig. 6. Influence of the aspect ratio of the short fibers on the fracture resistance ($\tilde{a} = 1000$ and $c = 0.5$).

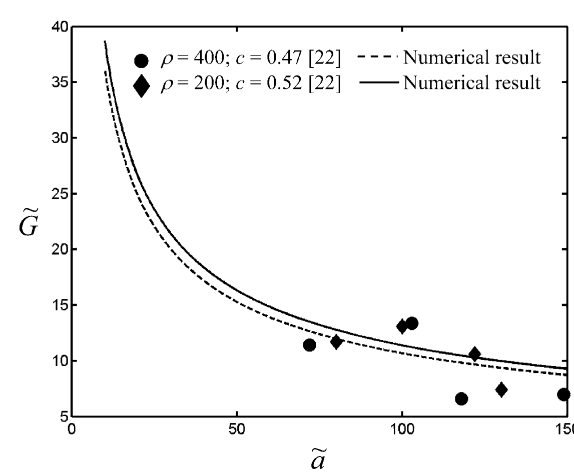

Fig. 7. The relationship between the fracture resistance and the initial crack length ($\tilde{k} = 104.2$).

increasing crack length when $\tilde{a}$ is small, and becomes somewhat independent to $\tilde{a}$ when it is relatively large. This size effect can also be attributed to the non-self-similar nature of the crack front. The numerical curve of the crack length effect was compared with the experimental result of the short fiber reinforced epoxy composites [22]. By using $\tilde{k}$ as an adjustable parameter the numerical solution fit with the experimental data quite well. However, this data fitting exercise does not constitute a fully definitive model and demonstrates only a proper framework for considering the crack size dependence of the fracture toughness, since when the fiber volume fraction is high, other toughening mechanisms can be significant and this model may no longer be valid.

In engineering practice, very often a simple regressed expression is useful. Rose [12] suggested that the fracture resistance of fiber-reinforced composites can be calculated as

$$\tilde{G} = 1 + \left(\tilde{K}^2 - 1\right)\frac{2r}{L} \tag{18}$$

where $\tilde{K}$ is the ratio of the toughness of the fiber to the toughness of the matrix. Similarly, if we assume that the effects of $\tilde{k}$ and c are of the form of power law, based on Eqs. (16) and (17), we may state that

$$\tilde{G} = 1 + \left(\tilde{k} - 1\right)^m \left(\frac{c}{\rho}\right)^n f_1(\rho, \tilde{a}) \tag{19}$$

where f_1 is a function to be determined. Since, if r, L, and a_0 are changed by the same factor, the model should be scalable, f_1 can be stated as $f_1 = \alpha(\rho/\tilde{a})^{\beta}$. Through the least square method, the numerical result can be regressed as

$$\tilde{G} = 1 + 1.83\left(\tilde{k} - 1\right)^{0.80} \left(\frac{c}{\rho}\right)^{0.42} \left(\frac{\rho}{\tilde{a}}\right)^{0.55} \tag{20}$$

In the range of parameters discussed above, the difference between the numerical solution and the regressed curve is less than 5%.

4. Conclusions

If the volume fraction of short fibers is relatively low or the traction distance is relatively small, the overall fracture toughness of short fiber reinforced composites is dominated by the behavior of a single fiber array. In this paper, the resistance to cleavage cracking of a regular array of short fibers was discussed in context of *R*-curve analysis. The internal friction between the fibers and the matrix was assumed constant, and the interaction among the fibers was neglected. When the energy release rate equals G_{matrix}, the crack begins to penetrate between the short fibers. The penetration depth of the cleavage front rises with the energy release rate. When the critical penetration depth is reached the crack advance becomes unstable before the fibers are fully pulled out, which leads to the final failure. The critical condition of the unstable crack propagation is determined by both of the first derivative and the second derivative of the strain energy. The following conclusions are drawn:

1. To study the overall fracture resistance, the crack front–fiber interaction must be taken account for. A vital microdamage factor governing the front behavior and the associated fracture work is the crack opening displacement along the short fibers.
2. The elastic properties of the matrix have little influence on the fracture toughness. The fracture toughness rises with the fiber volume fraction, the fiber length, and the effective strength of the fiber–matrix interface.
3. The fracture resistance is crack length dependent. The longer the initial crack, the smaller the critical energy release rate. However, when the crack length is much larger than the characteristic length of the fibers, this size effect becomes negligible.
4. The combined effects of these factors on the overall fracture resistance can be estimated through the regressed power-law expression.

Acknowledgements

This research was supported by the Firestone Research Initiative Fellowship. The authors are also grateful to Professor E. Pan for useful discussions.

References

[1] Hsueh CH. Modeling of elastic stress transfer in fiber-reinforced composites. Trends Polym Sci 1995;3:336–41.
[2] Sinclair I, Gregson PI. Structural performance of discontinuous metal matrix composites. Mater Sci Tech 1997;13: 709–26.
[3] Clyne TW. The effect of interfacial characteristics on the mechanical performance of particulate, fibrous and layered metal matrix composites—a review of some recent work. Key Eng Mater 1997;127:81–98.
[4] Krstic VD. Ceramic matrix composites—present status and future trends. Adv Mater Proc 1998;282:209–18.
[5] Sutherland LS, Soares CG. Review of probabilistic models of the strength of composite materials. Reliability Eng System Safety 1997;56:183–96.
[6] Nikpur K, Chen YF, Kardos JL. Fracture toughness of unidirectional short-fiber reinforced epoxy composites. Compos Sci Tech 1990;38:175–91.
[7] Ouyang C, Shah SP. Toughening of high strength cementitious

matrix reinforced by discontinuous short fibers. Cem Concr Res 1992;22:1201–15.

[8] Fernberg SP, Berglund LA. Bridging law and toughness characterization of CSM and SMC composites. Compos Sci Tech 2001;61:2445–54.

[9] Tjong SC, Xu SA, Li RKY, Mai YW. Short glass fiber-reinforced polyamide 6,6 composites toughened with maleated SEBS. Compos Sci Tech 2002;62:2017–27.

[10] Andersson J, Bergkvist H. Analysis of a nonlinear crack model. J Mech Phys Solids 1970;18:1–28.

[11] Mower TM, Argon AS. Experimental investigations of crack trapping in brittle heterogeneous solids. Mech Mater 1994;19:343–64.

[12] Rose LRF. Toughening due to crack–front interaction with a second-phase dispersion. Mech Mater 1987;6:11–15.

[13] Gao H, Rice JR. A first-order perturbation analysis of crack trapping by arrays of obstacles. J Appl Mech 1989;56:828–36.

[14] Bower AF, Ortiz M. A three-dimensional analysis of crack trapping and bridging by tough particles. J Mech Phys Solids 1991; 39:815–58.

[15] Bower AF, Ortiz M. The influence of grain size on the toughness of monolithic ceramics. Trans ASME 1993;115:228–36.

[16] Xu G, Bower AF, Ortiz M. The influence of crack trapping on the toughness of fiber reinforced composites. J Mech Phys Solids 1998;46:1815–33.

[17] Hellan K. Fracture mechanics. McGraw-Hill; 1984.

[18] Thomas S. Applied modeling and dimensional analysis. McGraw-Hill; 1997.

[19] Park SB, Lee BI, Lim YS. Experimental study on the engineering properties of carbon fiber reinforced cement composites. Cem Concr Res 1991;21:589–600.

[20] Lin GM, Lai JKL. Fracture mechanism in short fiber reinforced thermoplastic resin composites. J Mater Sci 1993;28:5240–6.

[21] Benthia N, Sheng J. Strength and toughness of cement mortars reinforced with micro-fibers of carbon, steel and polypropylene. In: Proc 2nd Canadian Symp Cem Concr, 1991.

[22] Nikpur K, Chen YF, Kardos JL. Fracture toughness of unidirectional short-fiber reinforced epoxy composites. Compos Sci Tech 1990;38:175–91.